大阪公立大学
Osaka Metropolitan University
学術情報リポジトリ

Amplitude death in time-delay nonlinear oscillators coupled by diffusive connections

メタデータ	言語: eng 出版者: 公開日: 2010-02-09 キーワード (Ja): キーワード (En): 作成者: Konishi, Keiji, Senda, Katsuhisa, Kokame, Hideki メールアドレス: 所属:
URL	http://hdl.handle.net/10466/6453

Amplitude death in time-delay nonlinear oscillators coupled by diffusive connections

Keiji Konishi,* Katsuhisa Senda, and Hideki Kokame
Department of Electrical and Information Systems, Osaka Prefecture University, 1-1 Gakuen-cho, Naka-ku, Sakai, Osaka, 599-8531 Japan
(Received 27 June 2008; published 25 November 2008)

This paper analyzes the stability of the amplitude death phenomenon that occurs in a pair of scalar time-delay nonlinear oscillators coupled by static, dynamic, and delayed connections. Stability analysis shows that static connections never induce death in time-delay oscillators. Further, for the case of dynamic and delayed connections, a simple instability condition under which death never occurs is derived. A systematic procedure for estimating the boundary curves of death regions is also provided. These analytical results are then verified by electronic circuit experiments.

DOI: 10.1103/PhysRevE.78.056216 PACS number(s): 05.45.Xt, 05.45.Gg, 02.30.Ks

I. INTRODUCTION

Various phenomena in coupled oscillators have been studied both from the viewpoint of academic interest as well as for practical applications [1–3]. Among these phenomena, the phenomenon of amplitude death, which is a diffusive-coupling induced stabilization of unstable fixed points, has been investigated for almost two decades [4,5]. It has been analytically proven that this phenomenon never occurs in identical coupled oscillators [5,6].

In 1998, Reddy, Sen, and Johnston reported that a time-delay connection can induce death even if the oscillators are identical [7]. The phenomenon of time-delay induced death has received considerable interest in the field of nonlinear physics [8], and has been observed in practical systems such as electronic circuits [9] and thermo-optical oscillators [10]. In addition, amplitude death has been studied analytically as follows: coupled simple limit cycle oscillators at Hopf bifurcation [11,12], odd-number property of death [6,13], ring-type coupled oscillators [14–17], death without delay coupling [18–20], distributed delay and asymmetric delay coupling [21,22], partial death in networks [23], and coupled chaotic oscillators [24,25].

Amplitude death is regarded as a stabilization of unstable behavior induced by a mutual interaction among two or more systems. Therefore, the clarification of the amplitude death mechanism is relevant to the elimination of unstable behavior in real coupled systems. In order to utilize death for such stabilization in practical situations, one has to design a mutual interaction that reliably induces death. However, there are two main problems associated with such a design. The first problem concerns how to select the type of mutual interactions and how to determine the coupling parameters. The second problem concerns how to deal with high-dimensional oscillators: most of the previous studies have only considered low-dimensional oscillators.

The main purpose of the present paper is to provide a solution for the above problems; in particular, this work focuses on three types of mutual interactions [5,7,18,19] and the time-delay nonlinear oscillator, which is a prototype model of infinite-dimensional systems [26]. The interactions considered here are static connections [5], dynamic connections [18,19], and delayed connections [7], which are easily implemented by physical systems such as electronic circuits, mechanical systems, and laser systems. Furthermore, time-delay systems [26,27] are widely used to model nonlinear phenomena such as chatter and chaos in metal cutting tools [28,29]. Thus the stabilization of time-delay systems remains an important issue for engineering applications [30].

The present paper investigates the stability of a pair of scalar time-delay nonlinear oscillators coupled by the three types of connections described above. A simple instability condition under which death never occurs is derived analytically, and a systematic procedure for estimating the boundary curves of the death region in the coupling parameter space is provided. Furthermore, these analytical results are then verified by electronic circuit experiments.

II. TIME-DELAY NONLINEAR OSCILLATORS

Time-delay nonlinear oscillators governed by delay differential equations, prototype models of infinite dimensional systems, have been widely used to investigate nonlinear phenomena in infinite-dimensional systems [26]. In recent years, time-delay nonlinear oscillators have further been used in practical applications, such as the anticipation of chaotic time series [31], chaotic synchronization [32–34], and communication schemes [35].

Consider two identical scalar time-delay oscillators

$$\dot{x}_1 = -\alpha x_1 + f(x_{1\tau}) + u_1,$$

$$\dot{x}_2 = -\alpha x_2 + f(x_{2\tau}) + u_2, \tag{1}$$

where $x_{1,2} \in \boldsymbol{R}$ are the scalar variables, $f:\boldsymbol{R} \to \boldsymbol{R}$ is a nonlinear scalar function, $x_{1,2\tau} := x_{1,2}(t-\tau)$ are the delayed variables, $u_{1,2} \in \boldsymbol{R}$ are coupling signals, and $\alpha > 0$ is a parameter. The symbol $\boldsymbol{R}$ is the set of real numbers. A fixed point of the individual nonlinear oscillator without coupling (i.e., $u_{1,2} \equiv 0$) is given by

*URL: http://www.eis.osakafu-u.ac.jp/

 ©2008 The American Physical Society

$$x^*:0 = -\alpha x^* + f(x^*). \tag{2}$$

These fixed points x^* are located at the intersections of $f(x)$ and αx. All of the fixed points x^* without coupling are assumed to be unstable throughout this paper.

Three types of diffusive connections are considered: static connections [32,33], dynamic connections [18,19], and delayed connections [6,7]. These connections are described by the following.

Static connection:

$$u_{1,2} = k(x_{1,2} - x_{2,1}). \tag{3}$$

Dynamic connection:

$$u_{1,2} = k(x_{1,2} - z),$$

$$\dot{z} = \gamma(x_1 + x_2 - 2z). \tag{4}$$

Delayed connection:

$$u_{1,2} = k(x_{1,2} - x_{2,1T}). \tag{5}$$

In the above, the delayed states are denoted by $x_{2,1T} := x_{2,1}(t-T)$, $\gamma > 0$ is a parameter, and $T \geqslant 0$ is the delay time for coupling. The coupling strength is denoted by $k \in \boldsymbol{R}$. These connections can change the stability of x^*; however, they cannot move the location of x^*. The amplitude death can be explained as a diffusive-connection induced stabilization of x^*.

III. STABILITY ANALYSIS

This section considers the stability of fixed points x^* in oscillators (1) coupled by connections (3)–(5). First, a simple sufficient condition under which death never occurs is derived. Second, a numerical procedure for estimating the boundary curve of the death region in parameter space is provided.

A. Simple instability condition

Applying linear stability analysis, the characteristic equation $g_1(\lambda)g_2(\lambda)=0$ is derived, where $g_1(\lambda)$ and $g_2(\lambda)$ depend on the connection type as follows.

Static connection:

$$g_1(\lambda) := \lambda + \alpha - \beta(x^*)e^{-\lambda\tau}, \tag{6}$$

$$g_2(\lambda) := \lambda + \alpha - 2k - \beta(x^*)e^{-\lambda\tau}. \tag{7}$$

Dynamic connection:

$$g_1(\lambda) := \lambda + \alpha - k - \beta(x^*)e^{-\lambda\tau}, \tag{8}$$

$$g_2(\lambda) := \det\begin{bmatrix} \lambda + \alpha - k - \beta(x^*)e^{-\lambda\tau} & 2k \\ -\gamma & \lambda + 2\gamma \end{bmatrix}. \tag{9}$$

Delayed connection:

$$g_1(\lambda) := \lambda + \alpha - k(1 - e^{-\lambda T}) - \beta(x^*)e^{-\lambda\tau}, \tag{10}$$

$$g_2(\lambda) := \lambda + \alpha - k(1 + e^{-\lambda T}) - \beta(x^*)e^{-\lambda\tau}. \tag{11}$$

Here $\beta(x^*) := \{df(x)/dx\}_{x=x^*}$ is the slope of $f(x)$ at x^*.

From these characteristic equations, it is straightforward to derive a simple instability condition [36].

Lemma 1. Amplitude death at the fixed point x^* never occurs in delayed nonlinear oscillators (1) coupled by a static connection (3) for any $k \in \boldsymbol{R}$.

Proof. It is noticed that $g_1(\lambda)=0$ is identical to the characteristic equation of the individual nonlinear oscillator without coupling. According to our assumption (i.e., x^* without coupling is unstable), $g_1(\lambda)=0$ has at least one root in the open right-half of the complex plane. Since $g_1(\lambda)$ does not depend on k, death never occurs for any $k \in \boldsymbol{R}$. ■

This lemma can be considered as an extension of Lemma 1 in Ref. [6] to delayed nonlinear oscillators. These results indicate that the static connection never induces amplitude death even if an individual oscillator includes a delayed state.

According to the previous results in Ref. [6], we have that if $\lim_{\lambda\to+\infty} h(\lambda) = +\infty$ and $h(0) < 0$, then there exists at least one positive real root for $h(\lambda)=0$ [40]. This fact yields the following two theorems.

Theorem 1. If $\alpha < \beta(x^*)$, then amplitude death at the fixed point x^* never occurs in delayed nonlinear oscillators (1) coupled by a dynamic connection (4) for any $k \in \boldsymbol{R}$, $\gamma > 0$, and $\tau \geqslant 0$.

Proof. It is clear that $\lim_{\lambda\to+\infty} g_2(\lambda) = +\infty$ and $g_2(0) = 2\gamma\{\alpha - \beta(x^*)\}$. Then $g_2(\lambda)=0$ has at least one positive real root for any $k \in \boldsymbol{R}, \gamma > 0, \tau \geqslant 0$, if $\alpha < \beta(x^*)$. ■

This theorem is also an extension of the previous result in Ref. [19].

Theorem 2. If $\alpha < \beta(x^*)$, then amplitude death at the fixed point x^* never occurs in delayed nonlinear oscillators (1) coupled by a delayed connection (5) for any $k \in \boldsymbol{R}$, $T > 0$, and $\tau \geqslant 0$.

Proof. It is clear that $\lim_{\lambda\to+\infty} g_1(\lambda) = +\infty$. $g_1(0) = \alpha - \beta(x^*)$ does not depend on k, T, τ. If $g_1(0) < 0$, then $g_1(\lambda) = 0$ has at least one positive real root. Amplitude death therefore never occurs for any k, T, τ, if $\alpha < \beta(x^*)$. ■

Theorem 2 is an extension of Theorem 2 in Ref. [6] to delayed nonlinear oscillators; hence, $\alpha < \beta(x^*)$ corresponds to the odd number property in [6]. Furthermore, it shall be noted that these theorems only describe sufficient conditions for avoiding death. In other words, when $\alpha > \beta(x^*)$, the theorems cannot guarantee whether or not death occurs.

Now we consider the case where there is only a single delayed nonlinear oscillator. In this case, death induced by delayed connection (5) and dynamic connection (4) can be regarded as a stabilization of delayed nonlinear systems by delayed feedback control and dynamic feedback control [37], respectively. From Theorems 1 and 2, we can easily derive the following result.

Corollary 1. Consider a single delayed-nonlinear oscillator

$$\dot{x} = -\alpha x + f(x_\tau) + u.$$

If $\alpha < \beta(x^*)$, then the fixed point x^* is not stabilized by delayed feedback control,

$$u = k(x - x_T),$$

for any $k \in \boldsymbol{R}, T > 0, \tau \geqslant 0$. In addition, if $\alpha < \beta(x^*)$, then x^* is not stabilized by dynamic feedback control,

$$u = k(x - z), \quad \dot{z} = \gamma(x - z)$$

for any $k \in \boldsymbol{R}, \gamma > 0, \tau \geqslant 0$.

B. Boundary curves of death region

This subsection estimates the boundary curves of the death region in parameter space for dynamic and delayed connections. For dynamic connection (4), $g_1(\lambda)g_2(\lambda)=0$ is investigated, where $g_1(\lambda)$ and $g_2(\lambda)$ are given by Eqs. (8) and (9), respectively. The fixed point x^* is stable if and only if all the roots of $g_1(\lambda)=0$ and $g_2(\lambda)=0$ lie in the open left-half of the complex plane. For simplicity, the two equations, $g_1(\lambda)=0$ and $g_2(\lambda)=0$, are considered separately.

According to the well-known condition in Ref. [38], the stability condition of $g_1(\lambda)=0$ is bounded by $k<\bar{k}$, where the upper boundary is given by

$$\bar{k} = \begin{cases} \alpha - \beta & \text{if } -\beta < 1/\tau, \\ \alpha - \beta\cos\zeta\tau & \text{if } -\beta > 1/\tau \end{cases} \tag{12}$$

in which ζ is a root of $-\beta\sin\zeta\tau=\zeta$ for $0<\zeta<\pi/\tau$.

Since the equation $g_2(\lambda)=0$ has an infinite number of roots, we examine only the movement of the roots in the complex plane. When roots cross the imaginary axis at $\pm i\omega$, they always satisfy $g_2(\pm i\omega)=0$. Therefore, the boundary for g_2 is one of the curves satisfying $g_2(\pm i\omega)=0$. Since $g_2(i\omega)=0$ is equivalent to $g_2(-i\omega)=0$, it is sufficient to examine $g_2(i\omega)=0$. The equation $g_2(i\omega)=0$ is divided into the real and imaginary parts:

$$2\gamma(\alpha - \beta\cos\omega\tau) - \omega(\omega + \beta\sin\omega\tau) = 0, \tag{13a}$$

$$\omega(\alpha - k - \beta\cos\omega\tau) + 2\gamma(\omega + \beta\sin\omega\tau) = 0. \tag{13b}$$

The algorithm to obtain the curves in the parameter space of (γ,k) is as follows: set a value for γ; obtain the positive real roots ω of Eq. (13a) by using the Newton method [41]; estimate the critical gain,

$$k = \frac{1}{\omega}\{2\gamma(\omega + \beta\sin\omega\tau) + \omega(\alpha - \beta\cos\omega\tau)\}, \tag{14}$$

where the roots ω are obtained by the preceding step; plot (γ,k); change the value of γ and then return to the first step. Furthermore, in order to investigate in which direction the roots cross the imaginary axis, one has to check the sign of real part of $d\lambda/dk$ at $\lambda=i\omega$:

$$\mathrm{Re}\left[\frac{\lambda}{2(\lambda+\gamma) + \alpha - k + \beta(\lambda\tau - 1 + 2\gamma\tau)e^{-\lambda\tau}}\right]_{\lambda=i\omega}, \tag{15}$$

where ω and k are the estimated values in the above procedure. With increasing k, a positive (negative) value of Eq. (15) corresponds to a pair of complex conjugate roots crossing the axis from left to right (right to left).

For delayed connection (5), $g_1(\lambda)g_2(\lambda)=0$ is investigated, where $g_1(\lambda)$ and $g_2(\lambda)$ are given by Eqs. (10) and (11), respectively: the two equations $g_1(\lambda)=0$ and $g_2(\lambda)=0$ are considered separately. As the equations $g_j(\lambda)=0$ for $j \in \{1,2\}$ have an infinite number of roots, we again examine only the movement of the roots in the complex plane. Since $g_j(i\omega)=0$ is equivalent to $g_j(-i\omega)=0$, it is sufficient to examine $g_j(i\omega)=0$. The equation $g_j(i\omega)=0$ is divided into the real and imaginary parts

$$(-1)^j\cos\omega T = A(k,\omega), \quad (-1)^{j+1}\sin\omega T = B(k,\omega), \tag{16}$$

where

$$A(k,\omega) := \frac{\alpha - k - \beta\cos\omega\tau}{k}, \quad B(k,\omega) := \frac{\omega + \beta\sin\omega\tau}{k}.$$

The algorithm to obtain the curves in the parameter space of (k,T) is as follows: set a value for k; estimate the positive real roots ω of

$$A(k,\omega)^2 + B(k,\omega)^2 = 1, \tag{17}$$

where this equation is derived from Eqs. (16) [42]; estimate the critical delay-time defined by $T_j(n)$ for $g_j(i\omega)=0$,

$$T_j(n) = \begin{cases} \dfrac{1}{\omega}\left[\arctan\left\{\dfrac{-B(k,\omega)}{A(k,\omega)}\right\} + 2n\pi\right] & \text{if } (-1)^j A(k,\omega) > 0, \\ \dfrac{1}{\omega}\left[\pi - \arctan\left\{\dfrac{B(k,\omega)}{A(k,\omega)}\right\} + 2n\pi\right] & \text{if } (-1)^j A(k,\omega) < 0, \end{cases} \tag{18}$$

for $n=0,1,\ldots$; plot $[k,T_j(n)]$; change the value of k and then return to the first step. Furthermore, one again has to check the sign of the real part of $d\lambda/dT$:

$$\mathrm{Re}\left[\frac{k\lambda e^{(-1)^{j+1}\lambda T}}{1 + (-1)^j kTe^{-\lambda T} + \beta\tau e^{-\lambda\tau}}\right]_{\lambda=i\omega, T=T_j(n)}. \tag{19}$$

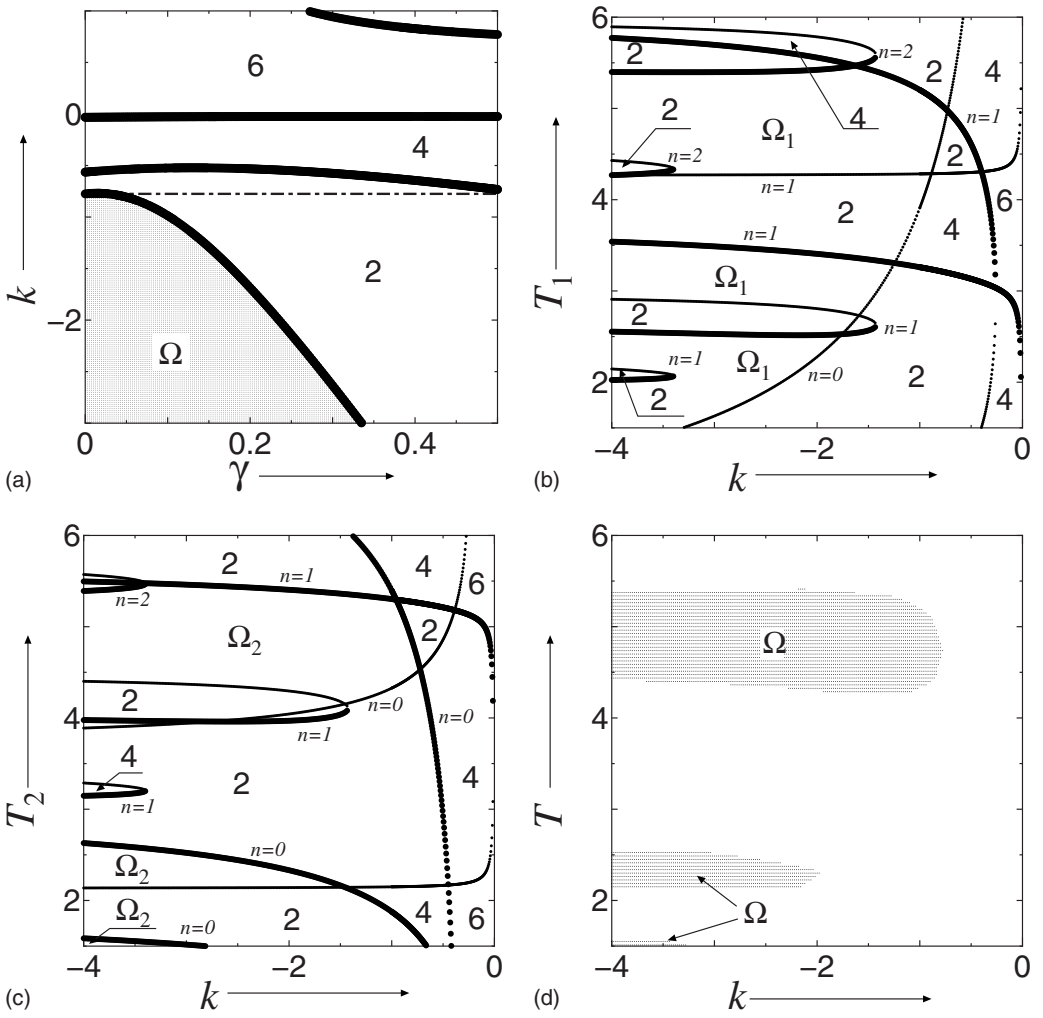


FIG. 1. Death regions Ω for the dynamic and delayed connections. A pair of complex conjugate roots crosses the imaginary axis from left to right (right to left) on the bold (thin) lines when k and $T_{1,2}$ increases. The numbers plotted in the figures denote the number of unstable roots. (a) Death region Ω for the dynamic connection, (b) boundary curves of $g_1(\lambda)=0$ for the delayed connection, (c) boundary curves of $g_2(\lambda)=0$ for the delayed connection, and (d) death region $\Omega=\Omega_1\cap\Omega_2$ for the delayed connection.

With increasing T_j, a positive (negative) value of Eq. (19) corresponds to a pair of complex conjugate roots crossing the axis from left to right (right to left).

C. A numerical example

This subsection provides a systematic procedure for estimating the death region in parameter space.

Step 1. The fixed point x^* satisfying Eq. (2) and the slopes of f at x^*, that is $\beta(x^*)$, are calculated. Note that if the value of $\beta(x^*)$ can be obtained, the fixed points, x^*, themselves are not required in this procedure.

Step 2. From Lemma 1, we notice that static connection (3) never induces death. In addition, Theorems 1 and 2 guarantee that the dynamic and delayed connections never induce death at fixed points x^* satisfying $\alpha<\beta(x^*)$. Accordingly, fixed points satisfying $\alpha>\beta(x^*)$ are analyzed in the next step.

Step 3. The boundary curves are plotted by the algorithm described in the preceding subsection. The number of unstable roots for $g_1(\lambda)=0$ and $g_2(\lambda)=0$ in the regions bounded by the curves is estimated by the sign of expressions (15) and (19). For the dynamic connection, the death region Ω is given by the set of parameters (γ,k) that satisfies $k<\bar{k}$ and lies within the regions bounded by curves (13). For the delayed connection, the death regions Ω are given by $\Omega=\Omega_1\cap\Omega_2$, where $\Omega_j:=\{(k,T):(k,T)$ lies in the regions bounded by the curves $T_j\}$.

It should be noted that step 2 chooses those fixed points that can potentially induce death on the basis of Theorems 1 and 2. Thus, it is not necessary for step 3 to calculate the boundary curves for fixed points without such potential. As a result, step 2 can significantly reduce the calculation time required for step 3. This saving is thus particularly noteworthy if the oscillator has a large number of fixed points.

As a numerical example of this procedure, consider the following nonlinear function [39]:

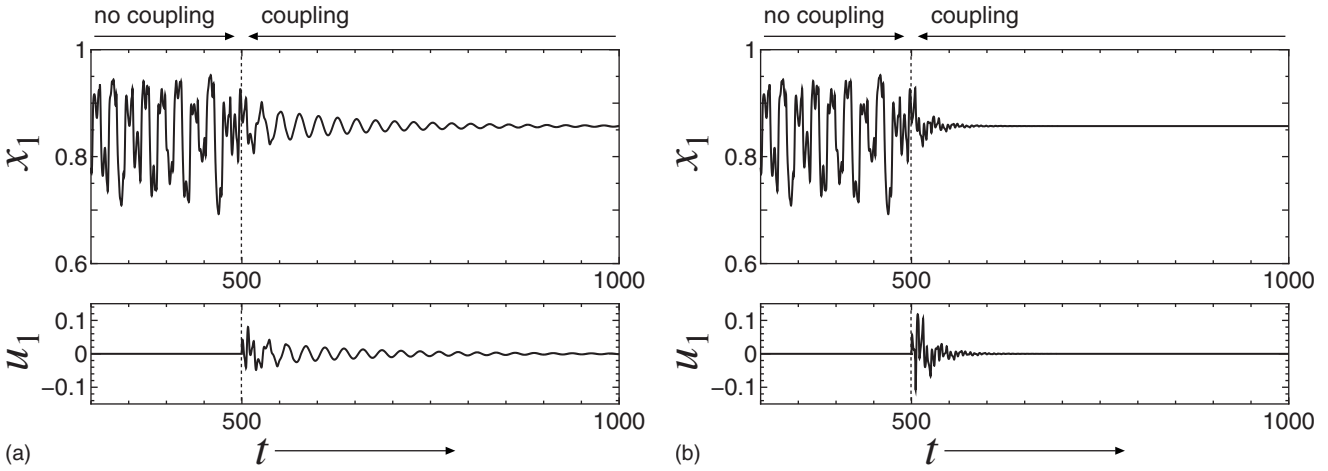


FIG. 2. Time series data $(x_1(t),u_1(t))$ just before and just after the coupling. (a) Dynamic connection ($\gamma=0.2$, $k=-2$). (b) Delayed connection ($k=-2$, $T=5.0$).

$$f(x)=\begin{cases}0 & \text{if } x\leqslant -4/3,\\ -1.8x-2.4 & \text{if } -4/3<x\leqslant -0.8,\\ 1.2x & \text{if } -0.8<x\leqslant 0.8,\\ -1.8x+2.4 & \text{if } 0.8<x\leqslant 4/3,\\ 0 & \text{if } x>4/3.\end{cases}$$

Hyperchaos occurs in Eq. (1) without coupling at $\alpha=1.0$ and $\tau=10.0$. In step 1, the three fixed points of f are easily calculated: $x^*=\pm 6/7$ and 0. Furthermore, the slopes at these points are given by $\beta(\pm 6/7)=-1.8$ and $\beta(0)=1.2$. Step 2 selects the fixed points $x^*=\pm 6/7$ as potential points, since these points do not satisfy the conditions of Theorems 1 and 2. In contrast, the slope $\beta(0)=1.2$ satisfies Theorems 1 and 2, and so dynamic (4) and delayed (5) connections never induce death at $x^*=0$ for any k, T, τ, γ. Step 3 draws the boundary curves, which are plotted in Fig. 1.

For the dynamic connection, the upper boundary is estimated as $\bar{k}=-0.7752$ from Eq. (12) [see the dashed-dotted line in Fig. 1(a)]. Thus, for $k<-0.7752$, no root of $g_1(\lambda)=0$ has positive real parts. Equation (13a) has the multiple roots ω; hence, there exist the multiple boundary curves. Further, it is easy to obtain the roots of $g_2(\lambda)=0$ at $k=0$ by solving the equation numerically: we have the six unstable roots at $k=0$. The number 6 plotted in Fig. 1(a) denotes the number of the unstable roots of $g_2(\lambda)=0$. Since the bold lines indicate that the sign of Eq. (15) is positive, we have that a pair of complex conjugate unstable roots crosses the imaginary axis from left to right as k increases. Therefore, once we numerically obtain the number of unstable roots at a point in parameter space (γ,k), the bold lines allow us to know the number at any point in the parameter space. By crossing the three bold lines, from the region labeled with 6, we can arrive the death region Ω which does not have any unstable roots.

For the delayed connection, the boundary curves T_1 and T_2 estimated by Eq. (18) and checked by the sign of expression (19) are plotted as shown in Figs. 1(b) and 1(c), respectively. Since Eq. (17) has the multiple roots ω; thus, there exist the multiple boundary curves for each integer n. A pair of complex conjugate roots crosses the imaginary axis from left to right (right to left) on the bold (thin) lines as $T_{1,2}$ increases. The numbers plotted in the figures denote the number of unstable roots. These numbers are also obtained in the same manner as the dynamic connection. From these figures, the death region $\Omega=\Omega_1\cap\Omega_2$ is obtained as shown in Fig. 1(d). It can be seen that a large death region exists at $T\simeq\tau/2$.

Figure 2(a) illustrates the time series data of the oscillators coupled by dynamic connection (4). The parameter γ is set to $\gamma=0.2$. The coupling strength k is changed from 0 to -2 at time $t=500$. The parameter set ($\gamma=0.2$, $k=-2$) is within the death region Ω in Fig. 1(a). The oscillators behave chaotically until $t=500$; thereafter, $x_1(t)$ and $u_1(t)$ converge on x^* and 0, respectively. The time series data for oscillators coupled by delayed connection (5) is illustrated in Fig. 2(b). The parameter set ($k=-2$, $T=5.0$) is within the death region in Fig. 1(d). After the coupling, $x_1(t)$ and $u_1(t)$ converge on x^* and 0, respectively.

On the basis of these results, the two connections are compared from practical viewpoints. The death region for the dynamic connection is like a vast continent in the parameter space; hence, death is robust for parameter variations. On the other hand, the region for the delayed connection consists of a few narrow strips: death is sensitive to parameter variations. Furthermore, the systematic procedure to estimate the boundary curves for the dynamic connection is

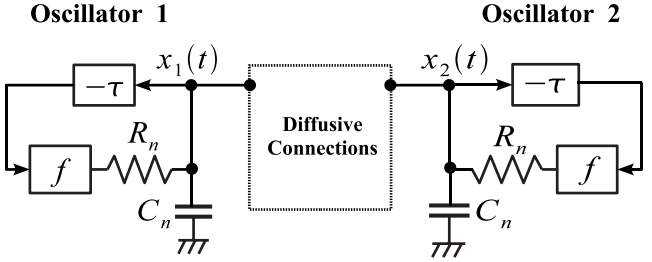


FIG. 3. Two identical time-delay nonlinear oscillators coupled by a connection circuit.

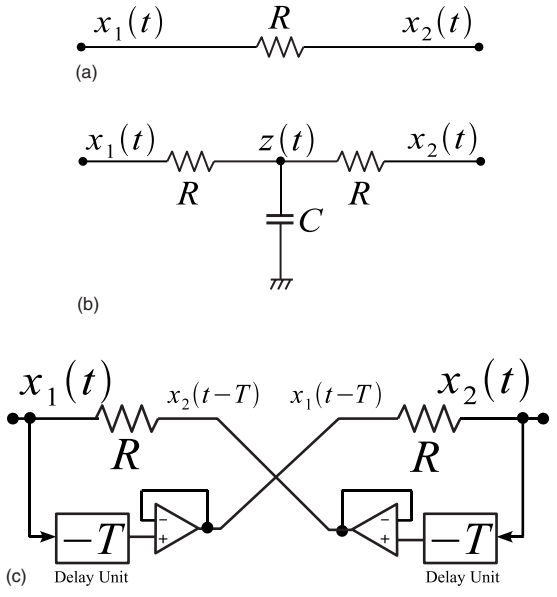


FIG. 4. Connection circuits realizing the three types of diffusive connections. (a) Static connection circuit, (b) dynamic connection circuit, and (c) delayed connection circuit.

simpler than that for the delayed connection. From these comparisons, it can be concluded that the dynamic connection is superior to the delayed connection for real situations. For real systems in which the dynamic connection can easily be realized (e.g., electric systems and mechanical systems), a system designer should consider exploiting the dynamic connection type in order to obtain death. However, for some real systems (e.g., laser systems), the designer may have no choice other than to use a delayed connection. In such cases, with reference to the above results, the designer has to adjust the delay time in the connection carefully.

IV. ELECTRONIC CIRCUIT EXPERIMENTS

A. Time-delay nonlinear oscillators

Two identical time-delay nonlinear oscillators coupled by diffusive connections are illustrated in Fig. 3. In the figure $x_i(t)$ denotes the voltage of oscillator i, $i=1,2$. The boxes labeled $-\tau$ and f are the time delay and nonlinear function units, respectively. These units are almost the same as a previous study [31]: the present paper employs MN3011 as a bucket brigade delay line for the time delay unit and 2SC1815 as a switching element in the nonlinear function unit. These oscillators are governed by

$$C_n\frac{dx_1(t)}{dt} = \frac{1}{R_n}\{f(x_1(t-\tau)) - x_1(t)\} + u_1(t),$$

$$C_n\frac{dx_2(t)}{dt} = \frac{1}{R_n}\{f(x_2(t-\tau)) - x_2(t)\} + u_2(t), \qquad (20)$$

where R_n, C_n are a resistor and capacitor, respectively. The coupling terms $u_i(t)$, $i=1,2$, are the currents from the connection circuit to the oscillators. The connection circuits for the three-type connections are sketched in Fig. 4, and are governed as follows.

Static connection:

$$u_{1,2}(t) = -\frac{1}{R}\{x_{1,2}(t) - x_{2,1}(t)\}. \qquad (21)$$

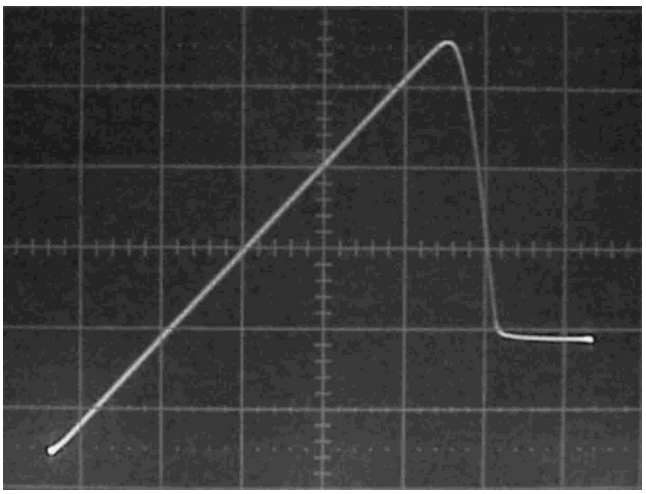
Dynamic connection:

$$u_{1,2}(t) = -\frac{1}{R}\{x_{1,2}(t) - z(t)\},$$

$$\frac{dz(t)}{dt} = \frac{1}{RC}\{x_1(t) + x_2(t) - 2z(t)\}. \qquad (22)$$

Delayed connection:

$$u_{1,2}(t) = -\frac{1}{R}\{x_{1,2}(t) - x_{2,1}(t-T)\}. \qquad (23)$$


(a)

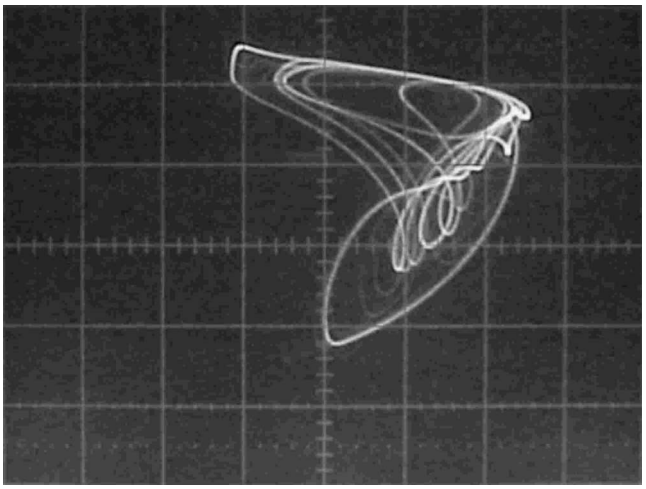

(b)

FIG. 5. Nonlinear function $f(x)$ and chaotic attractor. Horizontal axis: x (2V/div); vertical axis: $f(x)$ (2V/div). (a) $x-f(x)$ characteristic and (b) chaotic attractor for parameter set (A).

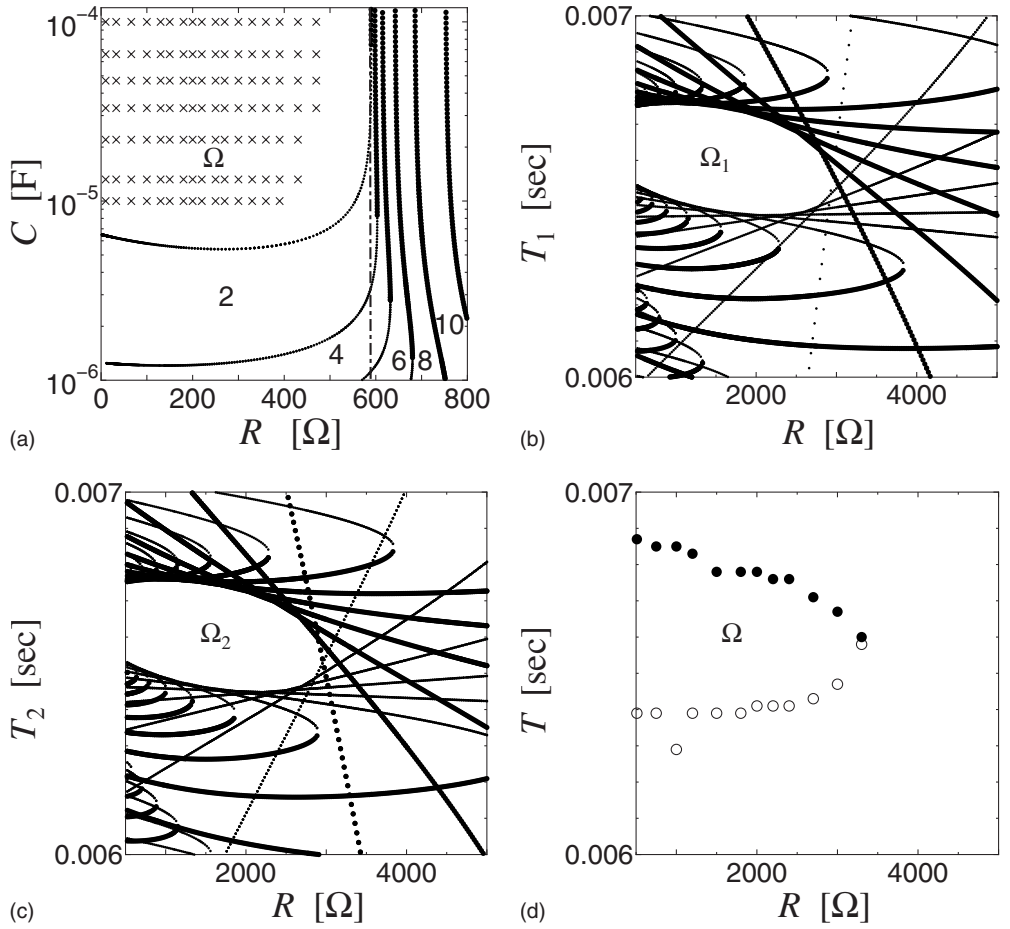


FIG. 6. Death regions Ω and boundary curves of oscillators (20) coupled by dynamic connection (22) and delayed connection (23). A pair of complex conjugate roots crosses the imaginary axis from left to right (right to left) on the bold (thin) lines when C and $T_{1,2}$ increases. (a) The × symbols plot where death occurs experimentally, and the boundary curves for the dynamic connection are also plotted. The numbers denote the number of unstable roots. (b), (c) The boundary curves of $g_{1,2}(\lambda)=0$ for the delayed connection are plotted. (d) The death induced by the delayed connection is observed experimentally. The symbol ● (○) indicates the upper (lower) limit of T for death.

In order to analyze the above circuits, we treat them as the dimensionless oscillators (1) on the basis of the following relations:

$$\tilde{t} := \frac{t}{R_n C_n}, \quad \dot{x}_{1,2} := \frac{dx_{1,2}(\tilde{t})}{d\tilde{t}}, \quad x_{1,2} := x_{1,2}(\tilde{t}),$$

$$x_{1,2\tau} := x_{1,2}(\tilde{t}-\tilde{\tau}), \quad \tilde{\tau} := \frac{\tau}{R_n C_n}, \quad u_{1,2} := u_{1,2}(\tilde{t}).$$

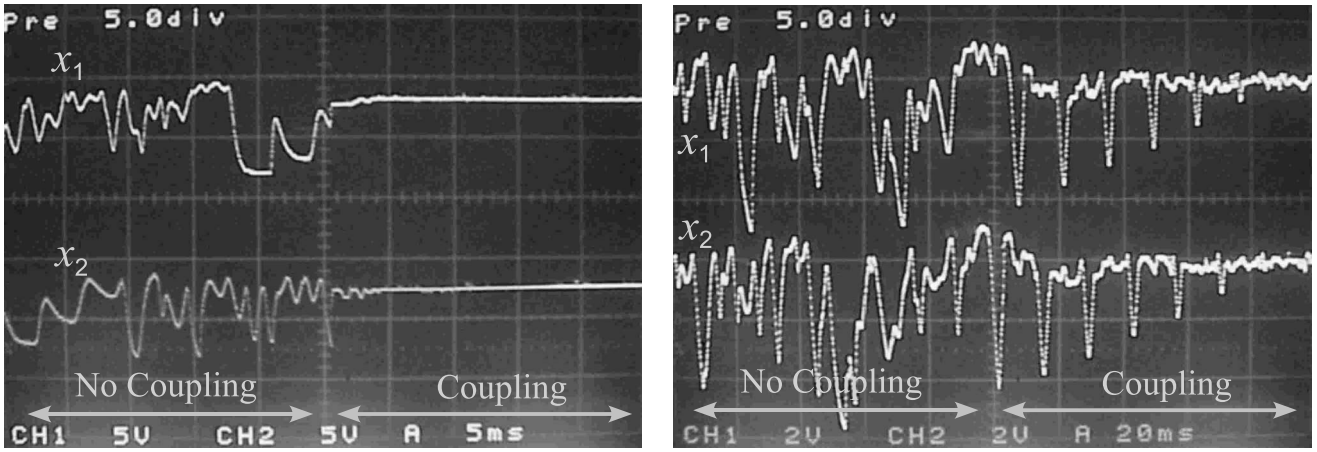
These relations show that circuit equation (20) is identical to Eq. (1) with $\alpha=1$. In addition, the other parameters and variables are described by the relations $k := -R_n/R$ for the static connection; $k := -R_n/R$, $z := z(\tilde{t})$, $\dot{z} := dz(\tilde{t})/d\tilde{t}$, $\gamma := R_n C_n/(RC)$ for the dynamic connection; $k := -R_n/R$, $x_{1,2T} := x_{1,2}(\tilde{t}-\tilde{T})$ and $\tilde{T} := T/(R_n C_n)$ for the delayed connection.

B. Experimental results

The input-output characteristic of the nonlinear function unit is shown in Fig. 5(a). From the characteristic, the fixed point x^* and the slope $\beta(x^*)$ are approximately estimated as $x^*=3.7$ V and $\beta(3.7)=-6.1$, respectively. Let us consider two parameter sets (A) $R_n=3.0$ kΩ, $C_n=0.1$ μF, $\tau=2.9$ ms; (B) $R_n=15.0$ kΩ, $C_n=0.1$ μF, $\tau=13.3$ ms. For both these sets, the individual oscillator exhibits chaotic behavior as shown in Fig. 5(b).

We have experimentally confirmed that death does not occur in oscillators (20) coupled by static connection (21) for any coupling resistor R. This result agrees with Lemma 1. The relation $\alpha=1>\beta(3.7)=-6.1$ obtained above does not satisfy Theorems 1 and 2; therefore, dynamic connection (22) and delayed connection (23) may induce death for the above experimental set up. The experimental studies shall be explained below.

Let us consider oscillators (20) with parameter set (A) coupled by dynamic connection (22). The death region and the boundary curves estimated by the procedure explained in the preceding section are plotted in $R-C$ parameter space as shown in Fig. 6(a). The symbol × denotes the parameter values (R, C) where death occurs experimentally. It can be seen that death region estimated by the systematic procedure agrees well with that obtained by circuit experiments.



(a) (b)

FIG. 7. Time series data $[x_i(t), i=1,2$ [V]] just before and just after the coupling. (a) Dynamic connection ($R=300\ \Omega$, $C=33\ \mu$F). (b) Delayed connection ($R=2000\ \Omega$, $T=6.66$ ms).

Oscillators (20) with parameter set (B) coupled by delayed connection (23) are also considered. The boundary curves of $g_{1,2}(\lambda)=0$ are plotted in $R-T_{1,2}$ parameter space as shown in Figs. 6(b) and 6(c). These curves are estimated by the procedure explained in the preceding section. Although there is not enough space to inscribe the number of unstable roots and the integer n due to being many curves, we can see the regions Ω_1 and Ω_2 clearly [43]. These regions are tangent to many curves; however, none of the curves cut across the regions. Figure 6(d) shows the death region as found by the circuit experiments. The symbol ● (○) indicates the upper (lower) limit of T for death. The death region estimated by the systematic procedure is almost the same as that obtained by circuit experiments. It should be noticed that this death region exists at $T \simeq \tau/2$. The similar result is also obtained in Fig. 1(d). This fact would be useful for design of delay time; however, the analytical relation between the death region and the delay time T is not clear at the present stage.

Figure 7(a) illustrates the time series data of the oscillators coupled by the dynamic connection circuit. The dynamic connection circuit is connected to the oscillators at the center of the figure. The oscillators behave chaotically until the center of the plot; thereafter, $x_{1,2}(t)$ converge on x^*. This convergence is the amplitude death observed in circuit experiments. The time series data for oscillators coupled by the delayed connection circuit is illustrated in Fig. 7(b). After the coupling, $x_{1,2}(t)$ gradually converge on x^*.

These experiments employ popular-priced circuit devices, which are not high precision (i.e., they have an error of several percent). Therefore, the experimental results imply that death occurred in time-delay nonlinear oscillators is a robust phenomenon to external noise and parameter mismatch.

V. CONCLUSION

This paper has investigated the stability of a pair of time-delay nonlinear oscillators coupled by static, dynamic, delayed connections. The static connection never induces death, even if an individual oscillator includes a delayed state. A simple instability condition under which death never occurs for dynamic or delayed connections has been derived. A systematic procedure for estimating the boundary curves of the death regions has also been provided. Furthermore, these analytical results have been experimentally verified by time-delay nonlinear circuits. Although this paper has dealt only with a pair of oscillators, it would be important to extend our results to large number of coupled oscillators. This extension is open for future work.

[1] T. Endo and S. Mori, IEEE Trans. Circuits Syst. **23**, 100 (1976).
[2] Y. Nishio and A. Ushida, IEEE Trans. Circuits Syst., I: Fundam. Theory Appl. **42**, 678 (1995).
[3] A. Pikovsky, M. Rosenblum, and J. Kurths, *Synchronization* (Cambridge University Press, Cambridge 2001).
[4] Y. Yamaguchi and H. Shimizu, Physica D **11**, 212 (1984).
[5] D. Aronson, G. Ermentout, and N. Kopell, Physica D **41**, 403 (1990).
[6] K. Konishi, Phys. Lett. A **341**, 401 (2005).
[7] D. V. Ramana Reddy, A. Sen, and G. L. Johnston, Phys. Rev. Lett. **80**, 5109 (1998).
[8] S. Strogatz, Nature (London) **394**, 316 (1998).
[9] D. V. Ramana Reddy, A. Sen, and G. L. Johnston, Phys. Rev. Lett. **85**, 3381 (2000).
[10] R. Herrero, M. Figueras, J. Rius, F. Pi, and G. Orriols, Phys. Rev. Lett. **84**, 5312 (2000).
[11] D. Reddy, A. Sen, and G. Johnston, Physica D **129**, 15 (1999).
[12] Y. Song, J. Wei, and Y. Yuan, J. Nonlinear Sci. **17**, 145 (2007).
[13] K. Konishi, Phys. Rev. E **67**, 017201 (2003).
[14] R. Dodla, A. Sen, and G. L. Johnston, Phys. Rev. E **69**, 056217 (2004).

[15] K. Konishi, Phys. Rev. E **70**, 066201 (2004).
[16] M. Mehta and A. Sen, Phys. Lett. A **355**, 202 (2006).
[17] J. Yang, Phys. Rev. E **76**, 016204 (2007).
[18] K. Konishi, Phys. Rev. E **68**, 067202 (2003).
[19] K. Konishi, Int. J. Bifurcation Chaos Appl. Sci. Eng. **17**, 2781 (2007).
[20] R. Karnatak, R. Ramaswamy, and A. Prasad, Phys. Rev. E **76**, 035201(R) (2007).
[21] F. M. Atay, Phys. Rev. Lett. **91**, 094101 (2003).
[22] C. U. Choe, V. Flunkert, P. Hövel, H. Benner, and E. Schöll, Phys. Rev. E **75**, 046206 (2007).
[23] F. Atay, Physica D **183**, 1 (2003).
[24] A. Prasad, Phys. Rev. E **72**, 056204 (2005).
[25] K. Konishi and H. Kokame, Phys. Lett. A **366**, 585 (2007).
[26] J. Farmer, Physica D **4**, 366 (1982).
[27] N. MacDonald, *Biological Delay Systems: Linear Stability Theory* (Cambridge University Press, Cambridge, 1989).
[28] F. Moon, *Dynamics and Manufacturing Processes* (J Wiley, New York, 1998).
[29] G. Radons and R. Neugebauer, *Nonlinear Dynamics of Production Systems* (Wiley-Vch, New York, 2004).
[30] H. Hu and Z. Wang, *Dynamics of Controlled Mechanical Systems with Delayed Feedback* (Springer, Berlin 2002).
[31] H. U. Voss, Phys. Rev. E **61**, 5115 (2000).
[32] M. J. Bünner and W. Just, Phys. Rev. E **58**, R4072 (1998).
[33] E. M. Shahverdiev and K. A. Shore, Phys. Rev. E **71**, 016201 (2005).
[34] S. Sano, A. Uchida, S. Yoshimori, and R. Roy, Phys. Rev. E **75**, 016207 (2007).
[35] W. H. Kye, M. Choi, C. M. Kim, and Y. J. Park, Phys. Rev. E **71**, 045202(R) (2005).
[36] K. Konishi and H. Kokame, *Proceedings of International Symposium on Nonlinear Theory and its Applications* (IEICE, Tokyo, 2007), pp. 389–392.
[37] A. Namajūnas, K. Pyragas, and A. Tamaševičius, Phys. Lett. A **204**, 255 (1995).
[38] J. Hale and S. Lunel, *Introduction to Functional Differential Equations* (Springer-Verlag, New York, 1993).
[39] D. V. Senthilkumar and M. Lakshmanan, Phys. Rev. E **71**, 016211 (2005).
[40] If the existence of complex root for $h(\lambda)=0$ were considered, one should treat λ as a complex number. However, this section proves only that there exists at least one positive real root for $h(\lambda)=0$. Therefore, it is sufficient to treat λ as a real number.
[41] The several roots ω are obtained by solving Eq. (13a). The subsequent steps of the algorithm and the sign check [i.e., Eq. (15)] are done for each root. As a result, the number of roots is identical to that of the curves at γ set in the first step. This is the reason why the multiple curves are obtained from single Eq. (14).
[42] Equation (17) has the several roots ω. The subsequent steps of the algorithm and the sign check [i.e., Eq. (19)] are done for each root; hence, at k set in the first step, the number of the roots is identical to that of the curves identified by the index n. This is the reason why there are the multiple curves for each n.
[43] If these figures are enlarged, it is possible to inscribe the number and the integer n obtained from the numerical data computed by the procedure. However, such enlarged figures cannot capture the whole death region. Since the aim of showing Figs. 6(b) and 6(c) is to compare the region computed by the numerical procedure with the region obtained by the circuit experiments, the number and the integer are ignored.